COSMIC RAYS DIFFUSION IN THE DYNAMIC MILKY WAY: MODEL, MEASUREMENT AND TERRESTRIAL EFFECTS

NIR J. SHAVIV

Racah Institute of Physics, Hebrew University
Jerusalem, 91904, Israel
E-mail: shaviv@phys.huji.ac.il

We study the problem of cosmic ray diffusion in the Milky Way while considering the galactic spiral arm dynamics. Once this new ingredient is added to cosmic ray diffusion models, we find that the cosmic ray flux reaching the solar system should increase periodically with each passage of a spiral arm. We continue with studying the meteoritic exposure ages and find that a record of past crossings of the arms can be extracted. We then briefly review recent evidence which links cosmic rays to climatic change on Earth. Given the suspected link, we argue that spiral arm passages are responsible for the periodic appearance of ice age epochs on Earth. This hypothesis is supported with a clear correlation between ice age epochs and the meteoritic record and also between longer term activity in the Milky Way and glacial activity on Earth. More speculatively, the last such passage may have been partially responsible for the demise of the dinosaurs.

1. Introduction

Most cosmic rays (CRs), with the possible exception of extremely high energies, are believed to originate from supernova (SN) remnants[1,2]. This is also supported by direct observational evidence[3]. Moreover, most SNe in spiral galaxies like our own are those which originate from massive stars, thus, they predominantly reside in the spiral arms, where most massive stars are born and shortly thereafter explode as SNe[4]. Indeed, high contrasts in the non-thermal radio emission are observed between the spiral arms and disks of external galaxies. Assuming equipartition between the CR energy density and the magnetic field, a CR energy density contrast can be inferred. In some cases, a lower limit of 5 can be placed for this ratio[5]. Thus, while modeling the diffusion of cosmic rays in the galaxy, we should take into consideration the non-axisymmetric nature of the cosmic ray source.

We first construct a diffusion model which considers the spiral arms as

the primary source of cosmic rays. We then continue with a study of the exposure ages of meteors which hide within them the history of the cosmic ray flux. As we shall soon see, this record registered the past half dozen spiral arm passages.

Quite unrelated, or so it may seem at first, there are indications that solar activity is responsible for at least some climatic variability on time scales ranging from days to millennia[6−15]. This link appears to be related to our topic of cosmic rays, since circumstantial evidence indicates that the observed solar-climate link could be though solar wind modulation of the cosmic rays flux (CRF)[13−15]. This is not unreasonable considering that the CRF governs the tropospheric ionization rate[16]. In particular, if was found that the low latitude cloud cover variations are in sync with the variable CRF reaching Earth, while the inverse of both signals lag by typically half a year after the solar activity[17].

Thus, if indeed climatic effects arise from *extrinsic CRF* variability induced by solar wind modulation, then also the much larger *intrinsic* variations in the CRF reaching the solar system should be a source of climatic effects. In particular, low altitude clouds have a net cooling effect, such that we should expect a colder climate while we are in the cosmic ray wake of spiral arms. This was shown to be supported by various data[18], and we bring here a more elaborate description. A complete unabridged version can be found in Shaviv[19] with the exception of the possible relation between cosmic rays and the demise of the dinosaurs, which appears here for the first time.

2. Diffusion in a Dynamic Galaxy

To estimate the variable CRF expected while the solar system orbits the galaxy, we construct a simple diffusion model which considers that the CR sources reside in the Galactic spiral arms. We expand the basic CR diffusion models (e.g., ref. [2]) to include a source distribution located in the Galactic spiral arms. Namely, we replace a homogeneous disk with an arm geometry as given by Taylor & Cordes[20], and solve the time dependent diffusion problem (see fig. 1). To take into account the "Orion spur"[21], in which the Sun currently resides, we add an arm "segment" at our present location. Since the density of HII regions in this spur is roughly half of the density in the real nearby arms[21], we assume it to have half the typical CR sources as the main arms. We integrate the CR sources assuming a diffusion coefficient of $D = 10^{28}\mathrm{cm}^2/\mathrm{sec}$, which is a typical value obtained

in diffusion models for the CRs[2,22,23]. We also assume a halo half-width of 2kpc, which again is a typical value obtained in diffusion models[2], but more importantly, we reproduce with it the ^{10}Be survival fraction[24]. Thus, the only free parameter in the model is the angular velocity $\Omega_\odot - \Omega_p$ around the Galaxy of the solar system *relative* to the Spiral arm pattern speed, which is later adopted using observations. Results of the model are depicted in fig. 2. For the nominal values chosen in our diffusion model and the particular pattern speed which will soon be shown to fit various data, the expected CRF changes from about 25% of the current day CRF to about 135%. Moreover, the average CRF obtained in units of today's CRF is 76%. This is consistent with measurements showing that the average CRF over the period 150-700 Myr before present (BP), was about 28% lower than the current day CRF[25].

Interestingly, the temporal behavior is both skewed and lagging after the spiral arm passages. The lag arises because the spiral arms are defined through the free electron distribution. However the CRs are emitted from SNe which on average occur roughly 15 Myr after the average ionizing photons are emitted. The skewness arises because it takes time for the CRs to diffuse after they are emitted. As a result, before the region of a given star reaches an arm, the CR density is low since no CRs were recently injected in that region and the sole flux is of CRs that succeed to diffuse to the region from large distances. After the region crosses the spiral arm, the CR density is larger since locally there was a recent injection of new CRs which only slowly disperse. This typically introduces a 10 Myr lag in the flux, totaling about 25 Myr with the SN delay. This lag is actually observed in the synchrotron emission from M51, which shows a peaked emission trailing the spiral arms[1].

The spiral pattern speed of the Milky Way has not yet been reasonably determined through astronomical observations. Nevertheless, a survey of the literature[19] reveals that almost all observational determinations cluster either around $\Omega_\odot - \Omega_p \approx 9$ to 13 (km s^{-1})/kpc or around $\Omega_\odot - \Omega_p \approx 2$ to 5 (km s^{-1})/kpc. In fact, one analysis[26] revealed that both $\Omega_\odot - \Omega_p = 5$ or 11.5 (km s^{-1})/kpc fit the data. However, if the spiral arms are a density wave[27], as is commonly believed[28], then the observations of the 4-arm spiral structure in HI outside the Galactic solar orbit[29] severely constrain the pattern speed to $\Omega_\odot - \Omega_p \gtrsim 9.1 \pm 2.4$ (km s^{-1})/kpc, since the four arm density wave spiral cannot extend beyond the outer 4 to 1 Lindblad resonance[19]. We therefore expect the spiral pattern speed obtained to coincide with one of the two aforementioned ranges, with a strong theoretical

argumentation favoring the first range.

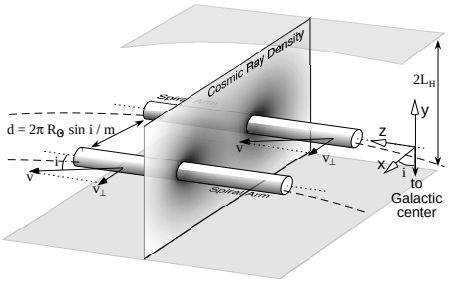

Figure 1. The components of the diffusion model constructed to estimate the Cosmic Ray flux variation. We assume for simplicity that the CR sources reside in Gaussian cross-sectioned spiral arms and that these are cylinders to first approximation. This is permissible since the pitch angle i of the spirals is small. The diffusion takes place in a slab of half width l_H, beyond which the diffusion coefficient is effectively infinite.

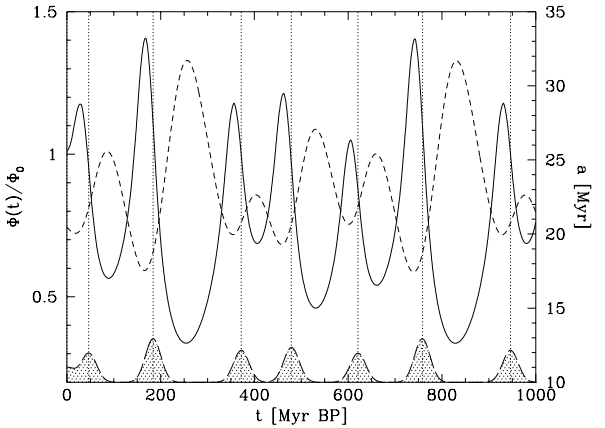

Figure 2. The cosmic-ray flux variability and age as a function of time for $D = 10^{28}$ cm^2/s and $l_H = 2$ kpc. The solid line is the cosmic-ray flux, the dashed line is the age of the cosmic rays as measured using the Be isotope ratio. The shaded regions at the bottom depict the location, relative amplitude (i.e., it is not normalized) and width of the spiral arms as defined through the free electron density in the Taylor and Cordes model. The peaks in the flux are lagging behind the spiral arm crosses due to the SN-HII lag. Moreover, the flux distribution is skewed towards later times.

3. The cosmic ray flux variability from meteorites

To validate the above prediction, that the CRF varied periodically, we require a direct "historic" record from which the actual time dependence of the CRF can be extracted. To find this record, we take a compilation of 74 Iron meteorites which were ^{41}K/^{40}K exposure dated[30]. CRF exposure dating (which measures the duration a given meteorite was exposed to CRs)

assumes that the CRF history was constant, such that a linear change in the integrated flux corresponds to a linear change in age. However, if the CRF is variable, the apparent exposure age will be distorted. Long periods during which the CRF is low would correspond to slow increases in the exposure age. Consequently, Fe meteorites with real ages within this low CRF period would cluster together since they will not have significantly different integrated exposures. Periods with higher CRFs will have the opposite effect and spread apart the exposure ages of meteorites. To avoid real clustering in the data (due to one parent body generating many meteorites), we remove all occurrences of Fe meteorites of the same classification that are separated by less than 100 Myr and replace them by the average. This leaves us with 42 meteorites. A graphical description of the method appears in fig. 3.

From inspection of fig. 4, it appears that the meteorites cluster with a period of 143 ± 10 Myr, or equivalently, $|\Omega_\odot - \Omega_p| = 11.0 \pm 0.8$ (km s^{-1})/kpc, which falls within the preferred range for the spiral arm pattern speed. If we fold the CR exposure ages over this period, we obtain the histogram in fig. 4. A K-S test yields a probability of 1.2% for generating this non-uniform signal from a uniform distribution. Moreover, fig. 4 also describes the prediction from the CR diffusion model. We see that the clustering is not in phase with the spiral arm crossing, but is with the correct phase and shape predicted by the CR model using the above pattern speed. A K-S test yields a 90% probability for generating it from the CR model distribution. Thus, we safely conclude that spiral arm passages modulate the CRF with a ~ 143 Myr period.

4. Do Cosmic rays affects the climate?

In 1959, Ney[16] suggested that the Galactic CR flux (CRF) reaching Earth could be affecting the climate since the CRF governs the ionization of the lower atmosphere, which in turn could be affecting cloud condensation. This, Ney postulated, could explain the observed climate variability synchronized with the solar cycle through the known modulation of the CRF by the solar wind. In 1991, Tinsley and Deen[13] brought first evidence in support. They showed that the Forbush events during which the CRF suddenly drops and gradually increases correlate with the Northern hemisphere Vorticity Area Index during winter. A much clearer and direct link was subsequently found in the form of an intriguing correlation between cloud cover and the CRF reaching Earth[15]. It was later shown to be cor-

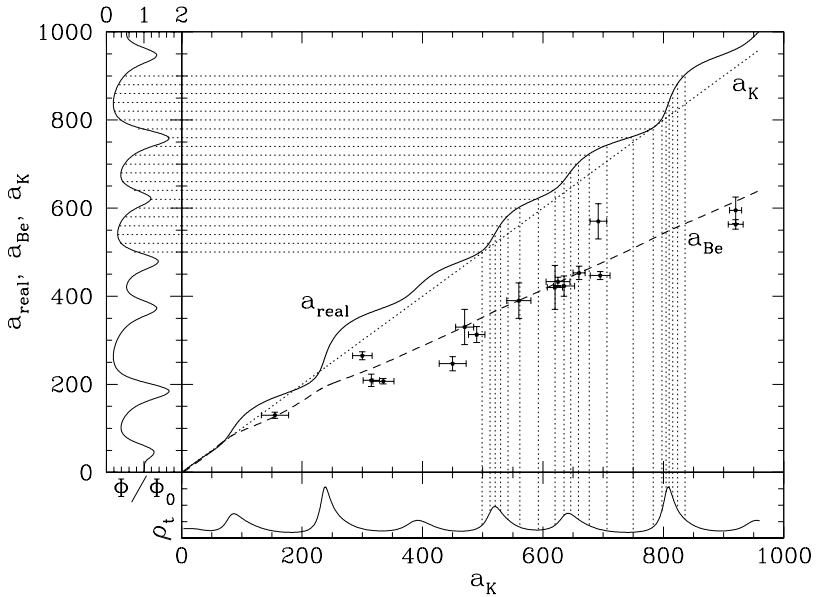

Figure 3. Theoretical comparison between different exposure ages of Iron meteorites and their real age. Plotted as a function of the Potassium exposure age ($a_{\rm K}$) are the real age ($a_{\rm real}$, in solid line) and a non-Potassium exposure age ($a_{\rm Be}$, such as using $^{10}{\rm B}/^{21}{\rm Ne}$ dating, with a dashed line), and $a_{\rm K}$ (using a dotted line, with a unit slope). Also plotted are the predicted CRF relative to the present flux (Φ/Φ_0) as a function of $a_{\rm real}$, and ρ_t–the (unnormalized) expected number of Potassium exposure ages per unit time, as a function of $a_{\rm K}$. A histogram of $a_{\rm K}$ should be proportional to ρ_t. The horizontal and vertical dotted lines describe how ρ_t is related to the relation between $a_{\rm real}$ and $a_{\rm K}$—equally spaced intervals in real time are translated into variable intervals in a_K, thereby forming clusters or gaps in $a_{\rm K}$. The graph of $a_{\rm Be}$ vs. $a_{\rm K}$ demonstrates that comparing the different exposure ages is useful to extract recent flux changes (which determine the slope of the graph). On the other hand, the graph of ρ_t demonstrates that a histogram of a_K is useful to extract the cyclic variations in the CRF, but not for secular or recent ones. The points with the error bars are about two dozen meteorites which where have both Be and K exposure dating.

related with the low altitude cloud cover (LACC) in particular, which is known to reduce the average global temperature[31,17].

The apparent CRF-LACC link was found through CRF modulation induced by the variable solar wind[15]. If this link is indeed genuine, then long term changes in the CRF induced by spiral arm crossing are too expected to episodically increase the average LACC, thereby reducing the average global temperature and triggering an ice-age epoch (IAE). We shall assume this link to be bona fide and study its consequences, though one should

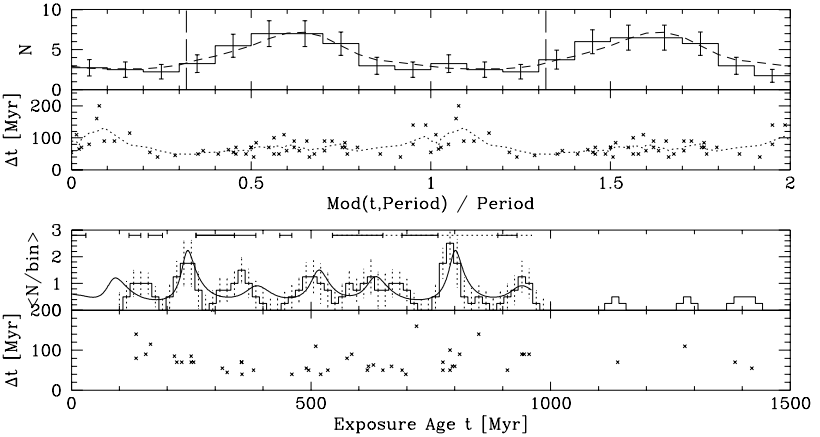

Figure 4. Histogram of the Iron meteorites' exposure ages. The lowest panel marks the a_K ages on the x-axis and the quoted age error on the y-axis. Even by eye, the ages appear to cluster periodically. The second panel is a 1:2:1 averaged histogram of meteorites with a quoted age determination error smaller than 100 Myr, showing more clearly the clustering peaks. Altogether, there are 6 peaks from 210 to 930 Myr BP. The period that best fits the data is 143 ± 10 Myr. The third panel is similar to the first one, with the exception that the data is folded over the periodicity found. It therefore emphasizes the periodicity. A Kolmogorov-Smirnov test shows that a homogeneous distribution could generate such a non-homogeneous distribution in only 1.2% of a sample of random realization. Namely, the signal appears to be real. This is further supported with the behavior of the exposure age errors, which supply an additional consistency check. If the distribution is intrinsically inhomogeneous, the points that fill in the gaps should on average have a larger measurement error (as it is 'easier' for these points to wonder into those gaps accidentally, thus forming a bias). This effect is portrayed by the dotted line in the panel, which plots the average error as a function of phase—as expected, the points within the trough have a larger error on average.

bear in mind that this issue still highly debated.

The apparent effect is on LACC (< 3.2 km), and therefore arises from relatively high energy CRs ($\gtrsim$10 GeV/nucleon). This CRF can reach equatorial latitudes, in agreement with observations showing a CRF-LACC correlation also near the equator[17]. Thus, when estimating the CRF-LACC forcing, the relevant flux is that of CRs that reach low magnetic latitude stations and that has a high energy cut-off. The flux measured at the University of Chicago Neutron Monitor Stations in Haleakala, Hawaii and Huancayo, Peru is probably a fair measurement of the flux affecting the LACC. Both stations are at an altitude of about 3 km and relatively close to the magnetic equator (rigidity cutoff of 12.9 GeV). The relative change in the CRF for the period 1982-1987 at Haleakala and Huancayo[32] is about

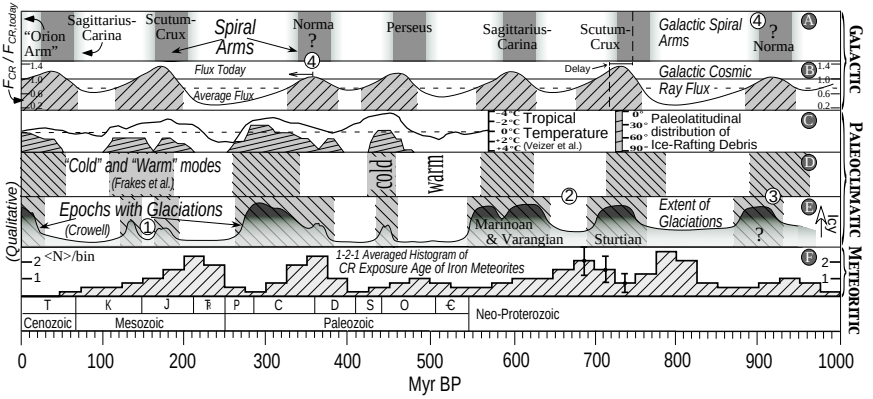

Figure 5. Earth's recent history. The top panel describes past crossings of the Galactic spiral arms assuming a relative pattern speed of $\Omega_p - \Omega_\odot = -11.0$ (km s^{-1})/kpc(which best fits the IAEs). Note that the Norma arm's location is actually a logarithmic spiral extrapolation from its observations at somewhat smaller Galactic radii. The second panel describes the Galactic CRF reaching the solar system using the CR diffusion model, in units of the current day CRF. An important feature is that the flux distribution around each spiral arm is lagging behind spiral arm crossings. This can be seen with the hatched regions in the second panel, which qualitatively show when IAEs are predicted to occur if the critical CRF needed to trigger them is the average CRF. Two arrows point to the middle of the spiral crossing and to the expected mid-glaciation point. The third panel qualitatively describes the epochs during which Earth experienced ice-ages. By fine-tuning the actual pattern speed of the arms (relative to our motion) to best fit the IAEs, a compelling correlation arises between the two. The correlation does not have to be absolute since additional factors may affect the climate (e.g., continental structure, atmospheric composition, etc.). The bottom panel is a 1-2-1 smoothed histogram of the exposure ages of Fe/Ni meteors. The ages should cluster around epochs with a lower CRF flux.

7%, while the relative change in the LACC[17] is about 6%. Namely, to *first approximation*, there is apparently a roughly linear relation between the relevant CRF and LACC.

Next, a 1% *relative* change in the global LACC corresponds[17] to a net effective reduction of the solar flux of $\Delta F_\odot \sim -0.17$ W/m^2. The relation between radiation driving and global temperature change is poorly known. Typical values[33] are $\Delta T/\Delta F_\odot = 0.7 - 1.0°\mathrm{K}/(\mathrm{W\ m}^{-2})$. We take a nominal value of $0.85°\mathrm{K}/(\mathrm{W\ m}^{-2})$.

Thus, changing the CRF by $\pm 1\%$ would correspond to a nominal change of $\mp 0.14°$K. For the nominal values chosen in our diffusion model, the expected CRF changes from about 25% of the current day CRF to about 135%. This corresponds to a temperature change of about $+10°$K to $-5°$K, relative to today's temperature. This range is sufficient to markably help

or hinder Earth from entering an IAE.

5. Ice Age Epochs and Spiral Passages

Extensive summaries of IAEs on Earth can be found in Crowell[34] and Frakes et al.[35]. Those of the past Eon are summarized in fig. 5. The nature of some of the IAEs is well understood while others are sketchy in detail. The main uncertainties are noted in fig. 5. For example, it is unclear to what extent can the milder mid-Mesozoic glaciations be placed on the same footing as other IAEs, nor is it clear to what extent can the period around 700 Myr BP be called a warm period since glaciations were present, though probably not to the same extent as the periods before or after. Thus, Crowell[34] concludes that the evidence is insufficient to claim a periodicity. On the other hand, Williams[36] claimed that a periodicity may be present. This was significantly elaborated upon by Frakes et al.[35].

Comparison between the CRF and the glaciations in the past 1 Gyr shows a compelling correlation (fig. 5). To quantify this correlation, we perform a χ^2 analysis. *To be conservative*, we do so with the Crowell data which is less regular. Also, we do not consider the possible IAE around 900 Myr, though it does correlate with a spiral arm crossing. For a given pattern speed, we predict the location of the spiral arms using the model. We find that a minimum is obtained for $\Omega_\odot - \Omega_p = 10.9 \pm 0.25$ (km s^{-1})/kpc, with $\chi^2_{min} = 1.1$ per degree of freedom (of which there are 5=6-1). We also repeat the analysis when we neglect the lag and again when we assume that the spiral arms are separated by 90° (as opposed to the somewhat asymmetric location obtained by Taylor and Cordes[20]). Both assumptions degrade the fit ($\chi^2_{min} = 2.9$ with no lag, and $\chi^2_{min} = 2.1$ with a symmetric arm location). Thus, the latter analysis assures that IAEs are more likely to be related to the spiral arms and not a more periodic phenomena, while the former helps assure that the CRs are more likely to be the cause, since they are predicted (and observed) to be lagged.

The previous analysis shows that to within the limitation of the uncertainties in the IAEs, the predictions of the CR diffusion model and the actual occurrences of IAE are consistent. To understand the significance of the result, we should also ask the question what is the probability that a random distribution of IAEs could generate a χ^2 result which is as small as previously obtained. To do so, glaciation epochs where randomly chosen. To mimic the effect that nearby glaciations might appear as one epoch, we bunch together glaciations that are separated by less than 60 Myrs (which

is roughly the smallest separation between observed glaciations epochs). The fraction of random configurations that surpass the χ^2 obtained for the best fit found before is of order 0.1% for *any* pattern speed. (If glaciations are not bunched, the fraction is about 100 times smaller, while it is about 5 times larger if the criterion for bunching is a separation of 100 Myrs or less). The fraction becomes roughly 6×10^{-5} (or a 4-σ fluctuation), to coincidentally fit the actual period seen in the Iron meteorites.

6. Star Formation Rate and Long Term Glacial Activity

Another interesting correlation between predicted CRF variability and glacial activity on Earth appears on a much longer time scale. Before 1 Gyr BP, there are no indications for any IAEs, except for periods around 2 - 2.5 Gyr BP (Huronian) and 3 Gyr BP (late Archean)[34]. This too has a good explanation within the picture presented. Different estimates to the Star formation rate (SFR) in the Milky Way (and therefore also to the CR production) point to a peak around 300 Myr BP, a significant dip between 1 and 2 Gyr BP (about a third of today's SFR) and a most significant peak at 2-3 Gyr BP (about twice as today's SFR)[37,38]. This would imply that at 300 Myr BP, a more prominent IAE should have occurred—explaining the large extent of the Carboniferous-Permian IAE. Between 1 and 2 Gyr BP, there should have been no glaciations and indeed none were seen. Last, IAEs should have also occurred 2 to 3 Gyr BP, which explains the Huronian and late-Archean IAEs. This can also be seen in fig. 6.

7. And the Dinosaurs?

Given the above scenario, cosmic rays may even be related to the disappearance of the dinosaurs. Indeed, it is most likely that the last of the dinosaurs saw the light of day during the K/T event, some 66 Myr ago, when a bolide hit the Yucatan peninsula (e.g., [39]). However, a careful study of fossils in N. America actually suggests that the number of dinosaur genera decreased by about a factor of 3 in the 10-15 Myr preceding the K/T event[40,41], and in Europe, the last dinosaurs appear to have disappeared 1-3 Myr before the K/T[42]. There are no widely accepted reason as to why this has happened. However, some point to the fact that the global climate cooled by typically 5-10°C in the 10-20 Myr preceding the K/T event[43,40,44] and that this cooling could have been an environmental stress that was too large for the dinosaurs to endure[43,40]. *If* this hypothesis is correct, namely, that most of the dinosaurs became extinct because the climate cooled quickly,

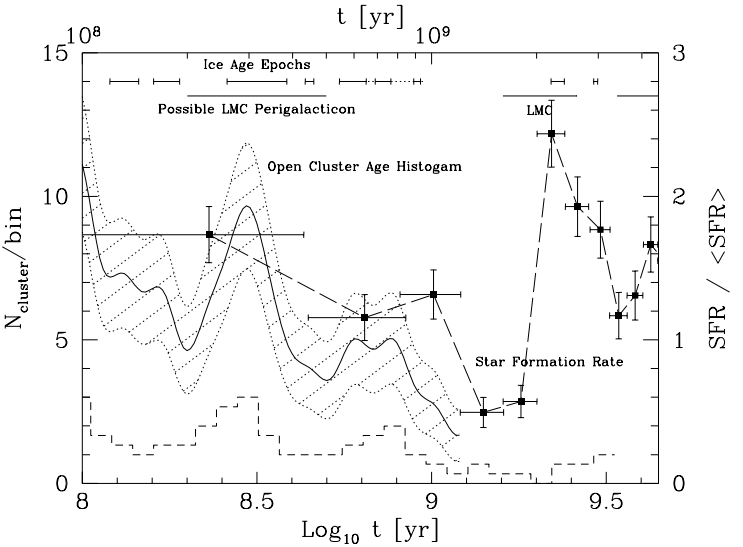

Figure 6. The history of the Star Formation Rate (SFR). The squares with error bars are the SFR calculated using chromospheric ages of nearby stars (Rocha Pinto et al.). These data are corrected for different selection biases and are binned into 0.4 Gyr bins. The line and hatched region describe a 1-2-1 average of the histogram of the ages of nearby open clusters using the Lotkin et al. catalog, and the expected 1-σ error bars. (These data are not corrected for selection effects). Since the clusters in the catalog are spread to cover two nearby spiral arms, the signal arising from the passage of spiral arms is smeared, such that the graph depicts a more global SFR activity (i.e., in our Galactic 'quadrant'). On longer time scales (1.5 Gyrs and more), the Galactic stirring is efficient enough for the data to reflect the SFR in the whole disk. The dashed histogram underneath is the same as the histogram above it, though only with clusters having a better age determination ($w > 1.0$, as defined in Lotkin et al.). There is a clear minimum in the SFR between 1 and 2 Gyr BP, and there are two prominent peaks around 0.3 and 2.2 Gyr BP. Interestingly, the LMC perigalacticon should have occurred sometime between 0.2 and 0.5 Gyr BP in the last passage, and between 1.6 and 2.6 Gyr before present in the previous passage. This would explain the peaks in activity seen. This is corroborated with evidence of a very high SFR in the LMC about 2 Gyrs BP and a dip at 0.7 - 2 Gyr BP. Also depicted are the periods during which glaciations were seen on Earth: The late Archean (3 Gyr) and mid-Proterozoic (2.2-2.4 Gyr BP) which correlate with the previous LMC perigalacticon passage (Gardiner 1994, Lin 1995) and the consequent SFR peak in the MW and LMC. The lack of glaciations in the interval 1 - 2 Gyr before present correlates with a clear minimum in activity in the MW (and LMC). Also, the particularly long Carboniferous-Permian glaciation, correlates with with the SFR peak at 300 Myr BP and the last LMC perigalacticon. The late Neo-Proterozoic ice ages correlate with a less clear SFR peak around 500-900 Myr BP.

then most of the extinction can be directly related to the fact that the solar system entered the Sagittarius-Carinae spiral arm during that period.

8. Summary

To conclude, we first considered that most CR sources reside in the Galactic spiral arms, and incorporated this fact into a cosmic ray diffusion model. Unsurprisingly, this model predicts a variable CRF. By analyzing the exposure ages in Iron meteorites, it was found that the cosmic ray flux history can be reconstructed. It was found to vary periodically, and it nicely agrees with the observations of the Galactic spiral arm pattern speed.

Next, if recent evidence linking the CRF to low altitude cloud cover on Earth is real, typical variations of $\mathcal{O}(10°\mathrm{K})$ are predicted from the variable CRF. Each spiral arm crossing, the average global temperature should reduce enough to trigger an IAE. The record of IAEs on Earth is fully consistent with the predicted and observed CRF variation—both in period and in phase. Next, the fit is also found to be better when the predicted lag in the mid-point of the IAEs after each crossing is included and when the actual asymmetric location of the arms is taken into account. Moreover, a random mechanism to generate the IAEs is excluded.

On a more speculative note, there is a curious correlation between the global cooling experienced on Earth at the end of the Cretaceous and the disappearance of the dinosaurs. If the the latter is related to climate change, it could be attributed to the solar system entering a spiral arm.

References

1. M. S. Longair, *High Energy Astrophysics*, 2nd ed., vol. 2 (Cambridge Univ. Press, Cambridge, 1994)
2. V. S. Berezinskiĭ, S. V. Bulanov, V. A. Dogiel, V. L. Ginzburg, V. S. Ptuskin, *Astrophysics of Cosmic Rays*, (North-Holland, Amsterdam, 1990)
3. N. Duric, In *Proceedings 232. WE-Heraeus Seminar, 22-25 May 2000, Bad Honnef, Germany. Edited by Elly M. Berkhuijsen, Rainer Beck, and Rene A. M. Walterbos. Shaker, Aachen, 2000*, p. 179 (2000).
4. P. M. Dragicevich, D. G. Blair, and R. R. Burman, *Mon. Not. Roy. Astr. Soc.*, **302**, 693 (1999).
5. N. Duric, *Astrophys. J.*, **304**, 96 (1986).
6. G. Bond et al., *Science*, **294**, 2130 (2001).
7. U. Neff, S. J. Burns, A. Mangnini, M. Mudelsee, D. Fleitmann, and A. Matter, *Nature*, **411**, 290 (2001).
8. D. A. Hodell, M. Brenner, J. H. Curtis, and T. Guilderson, *Science*, **292**, 1367 (2001).
9. E. Friis-Christensen and K. Lassen, *Science*, **254**, 698 (1991).
10. W. H. Soon, E. S. Posmentier, and S. L. Baliunas, *Astrophys. J.*, **472**, 891 (1996).
11. W. H. Soon, E. S. Posmentier, and S. L. Baliunas, *Annales Geophysicae*, **18**,

583 (2000).
12. J. Beer, W. Mende, and R. Stellmacher, *Quat. Sci. Rev.*, **19**, 403 (2000).
13. B. A. Tinsley and G. W. Deen, *J. Geophys. Res.*, **12**, 22283 (1991).
14. L. Y. Egorova, V. Ya. Vovk, and O. A. Troshichev, *J. Atmos. Solar-Terr. Phys.*, **62**, 955 (2000).
15. H. Svensmark, *Phys. Rev. Lett.*, **81**, 5027 (1998).
16. E. P. Ney, *Nature*, **183**, 451 (1959).
17. N. Marsh and H. Svensmark, *Sp. Sci. Rev.*, **94**, 215 (2000).
18. Shaviv, N. J., *Phys. Rev. Lett.*, **89**, 051102 (2002).
19. Shaviv, N. J., *New Astron.*, in press (2002).
20. J. H. Taylor and J. M. Cordes, *Astrophys. J.*, **411**, 674 (1993).
21. Y. M. Georgelin and Y. P. Georgelin, *Astron. Astrophy.*, **49**, 57 (1976).
22. W. R. Webber and A. Soutoul, *Astrophys. J.*, **506**, 335 (1998).
23. U. Lisenfeld, P. Alexander, G. G. Pooley, and T. Wilding, *Mon. Not. Roy. Astr. Soc.*, **281**, 301 (1996).
24. A. Lukasiak, P. Ferrando, F. B. McDonald, and W. R. Webber, *Astrophys. J.*, **423**, 426 (1994).
25. B. Lavielle, K. Marti, J. Jeannot, K. Nishiizumi, and M. Caffee, *Earth Plan. Sci. Lett.*, **170**, 93 (1999).
26. J. Palous, J. Ruprecht, O. B. Dluzhnevskaia, and T. Piskunov, *Astron. Astrophy.*, **61**, 27 (1977).
27. Lin C. C., Shu F. H., *Astrophys. J.***140**, 646 (1964).
28. J. Binney, S. Tremaine, *Galactic Dynamics*, (Princeton Univ. Press, Princeton, 1988)
29. L. Blitz, M. Fich, and S. Kulkarni, *Science*, **220**, 1233 (1983).
30. H. Voshage, H. Feldmann, *Earth Planet. Sci. Lett* **45**, 293 (1979).
31. V. Ramanathan, R. D. Cess, E. F. Harrison, P. Minnis, and B. R. Barkstron, *Science*, **243**, 57 (1989).
32. G. A. Bazilevskaya, *Sp. Sci. Rev.*, **94**, 25 (2000).
33. D. Rind and J. Overpeck, *Quat. Sci. Rev.*, **12**, 357 (1993).
34. J. C. Crowell, *Pre-Mesozoic Ice Ages: Their Bearing on Understanding the Climate System*, volume 192. Memoir Geological Society of America (1999).
35. L. A. Frakes, E. Francis, and J. I. Syktus, *Climate modes of the Phanerozoic; the history of the Earth's climate over the past 600 million years*. Cambridge: Cambridge University Press (1992).
36. G. E. Williams, *Earth and Plan. Sci. Lett.*, **26**, 361 (1975).
37. J. M. Scalo, In *Starbursts and Galaxy Evolution*, p. 445 (1987).
38. H. J. Rocha-Pinto, J. Scalo, W. J. Maciel, and C. Flynn, *Astron. Astrophy.*, **358**, 869 (2000).
39. van den Bergh S., Proc. Ast.. Soc. Pac., **106**, 689 (1994).
40. R. E. Sloan et al., *Science*, **232**, 629 (1986)
41. R. E. Sloan, J. K. Rigby Jr., L. van Valen, and L.-D., *Science*, **232**, 633 (1986).
42. B. Galbrun, *Earth Planet. Sci. Lett.*, **148**, 569 (1997).
43. D. M. McLean, *Science*, **201**, 401 (1978).
44. B. T. Huber, *Science*, **282**, 2199 (1998).